



Relative binding affinities of fluorobenzene ligands in cationic rhodium bisphosphine η^6 -fluorobenzene complexes probed using collision-induced dissociation

Sebastian D. Pike^{a,*}, Indrek Pernik^a, Robin Theron^b, J. Scott McIndoe^{b,*}, Andrew S. Weller^{a,*}

^a Department of Chemistry, Chemical Research Laboratories, Mansfield Road, Oxford OX1 3TA, UK

^b Department of Chemistry, University of Victoria, P.O. Box 3065, Victoria, BC V8W 3V6, Canada

ARTICLE INFO

Article history:

Received 19 July 2014

Received in revised form

12 August 2014

Accepted 14 August 2014

Available online 23 August 2014

Keywords:

Mass spectrometry

Fluorobenzene

Arene

Rhodium

Relative binding affinity

ABSTRACT

A range of cationic rhodium bisphosphine η^6 -fluorobenzene (fluorobenzenes = $C_6H_{6-n}F_n$, $n = 1-3$) and related complexes have been synthesized and characterized. These complexes act as useful organometallic precursors for catalysis or further synthetic elaboration. The relative binding affinity of the arene ligands has been investigated using Electrospray Ionisation Mass Spectrometry (ESI-MS) and two different collision-induced dissociation (CID) techniques. The influence of arene fluorination upon arene binding affinity is discussed as well as the comparison of different bis-phosphine ligands with regard to bite angle and phosphine substitution. We show that this simple technique allows fast and easy comparison of the binding affinity of arene ligands to cationic organometallic fragments.

© 2014 The Authors. Published by Elsevier B.V. This is an open access article under the CC BY license (<http://creativecommons.org/licenses/by/3.0/>).

Introduction

The study and development of catalytic processes mediated by transition-metal complexes has been, and remains, an area of intense academic and industrial interest [1]. For systems that operate via inner-sphere processes, a catalyst typically requires available vacant sites for the substrate to bind. Often these are masked by a labile ligand, i.e. they are “operationally unsaturated” [2], and ideally this masking ligand does not interfere with the progress of the catalytic process. We have recently developed the use of fluorobenzene-ligated $[Rh(\eta-C_6H_5F)(L)_2][BAR^F_4]$ complexes [$(L)_2$ = monodentate or bidentate phosphine, $Ar^F = 3,5-(CF_3)_2C_6H_3$] as precatalysts for hydroacylation [3,4], silane reduction of C–S bonds [5], Suzuki type C–C coupling via C–S activation [6], and the dehydrogenation of amine- and phosphine-boranes [7–11], as well as stoichiometric intramolecular C–H activation processes [12–14]. Some of these pre-catalysts have also been found to be bench-stable [3,4], while the bound arene can be substituted by solvents, such as acetone, to provide access to 16-electron $[Rh(L)_2(solvent)_2][BAR^F_4]$ complexes [4,6].

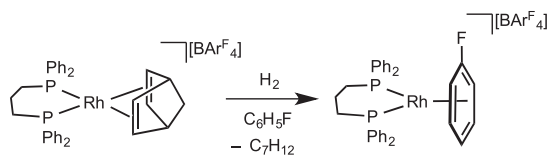
Many of these fluorobenzene complexes have been structurally characterized. The general synthetic route to their formation is hydrogenation of a strained bis-alkene ligand such as NBD (NBD = norbornadiene) in a precursor $[Rh(NBD)(L)_2][BAR^F_4]$ complex in the appropriate solvent, i.e. fluorobenzene (Scheme 1).

Remarkably, given the now widespread use of fluorobenzene (and to a lesser extent *ortho* difluorobenzene) as a solvent in organometallic chemistry there are, outside of those listed above, relatively few examples of isolated fluorobenzene complexes [15,16]. In some examples coordination through the fluorine atoms can occur rather than coordination through the π -system e.g. **A** (Scheme 2) [17–19], while η^2 -coordination of the arene is also possible given the appropriate electronic and steric environment is provided by the metal, e.g. **B** [20,21]. Fluorobenzene also acts as a ligand to main group species, e.g. $[Ga(\eta^6-C_6H_5F)_3]^+$ **C** [22] and post-transition metals, e.g. **D**. C–F activation of fluoroarenes has also been widely reported, and η^2 -coordinated intermediates are suggested to be involved in the process that forms M–F and M–aryl bonds [23]. Closely related to these weakly-bound fluoroarene complexes are zwitterionic species in which a $[BAR^F_4]^-$ anion coordinates with the metal through the arene ring, e.g. **E**. [24–26].

Given the broad range of complexes of general formula $[Rh(\eta-fluoroarene)(L)_2][BAR^F_4]$ reported by our group and others, and the use of these complexes in both catalysis and synthesis, we

* Corresponding authors.

E-mail address: andrew.weller@chem.ox.ac.uk (A.S. Weller).



Scheme 1. Example of the general synthetic routes to fluorobenzene complexes of the general formula $[\text{Rh}(\eta\text{-C}_6\text{H}_5\text{F})(\text{L})_2][\text{BAR}^{\text{F}}_4]$; ($\text{L}_2 = \text{Ph}_2\text{PCH}_2\text{CH}_2\text{CH}_2\text{PPh}_2$) [7].

were interested in a straightforward way of measuring the relative binding strength of fluorobenzene in a variety of complexes. For example, we have recently reported the strength of binding of fluorobenzene, relative to an alternative solvent complex, can be modified as a function of the bite angle [27,28] of the supporting chelating phosphine ligand in $[\text{Rh}(\eta\text{-C}_6\text{H}_5\text{F})(\text{L})_2][\text{BAR}^{\text{F}}_4]$ complexes where $\text{L} =$ chelating ligand, in which wider bite angle ligands promote equilibria that favour the solvent–species, $[\text{Rh}(\text{L})_2(\text{acetone})_2][\text{BAR}^{\text{F}}_4]$ [4]. As fluoroarenes are usually installed on metal centers to either stabilize a low-coordinate metal center or act as a masking ligand to reveal such a reactive center, a straightforward measure of the relative binding strengths of different fluoroarenes with the same metal fragment, or different metal fragments with the same fluoroarene, would be useful. Of course, equilibrium studies in solution can provide such information, however we were interested in developing other techniques that might complement such methods, and turned to ESI–MS to do this. Fluorobenzene is quite polar enough to permit the acquisition of high quality ESI mass spectra [29].

Mass spectrometry techniques have been previously used to study the binding affinities of fluorobenzenes with metal cations. Klippenstein, Dunbar and co-workers reported the coordination of fluorobenzenes with Cr^+ ions probed by radiative association kinetics in the gas-phase using Fourier transform ion cyclotron resonance mass spectrometry [30]. The energetics of the arene binding in the $[\text{Cr}(\text{fluorobenzene})]^+$ fragment were determined and showed that increasing fluorination results in weaker binding affinity. Previous studies have suggested that coordination to the π system of arenes by transition metals has a significant electrostatic component [31,32], and that additional fluorine substituents reduce the negative charge located across the π region so that in the

extreme case of hexafluorobenzene the π region has a partial positive charge.

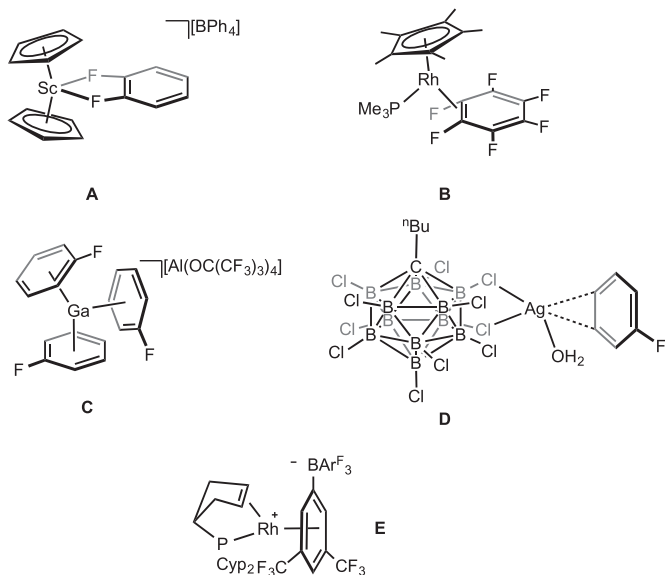
Other, more accessible for the synthetic chemist, mass spectrometric techniques can be used for determining relative binding strengths, for example tandem electrospray ionization mass spectrometers (ESI–MS/MS) have the capability to selectively fragment ions in a collision cell and determine the energetics of their dissociation [33,34]. More generally, ESI–MS is a useful technique for characterizing charged complexes in polar solvents, as it is a “soft” ionization technique and allows the parent ion to be observed with little or no fragmentation [35]. This property is particularly useful for studying weakly-bound, or transient, organometallic complexes [36,37] and can be coupled with inert atmosphere glove-box techniques in order to study air-sensitive complexes [38]. In this contribution we utilize Collision Induced Dissociation (CID) techniques to establish comparative binding affinities of various fluorobenzene ligands in a range of complexes $[\text{Rh}(\eta\text{-C}_6\text{H}_{6-x}\text{F}_x)(\text{L})_2]^+$ where the chelating phosphine (L) is also varied. We also correlate these results from ESI–MS with both ESI–MS/MS and solution-based equilibrium studies. In doing this we present ESI–MS as a simple and straightforward methodology for determining qualitative information on the relative binding strengths of the arenes. Quantification of ligand binding strength is a substantially more involved process that requires the use of energy-resolved threshold CID techniques that necessitate instrumentation that is not commercially available [39–41].

Results and discussion

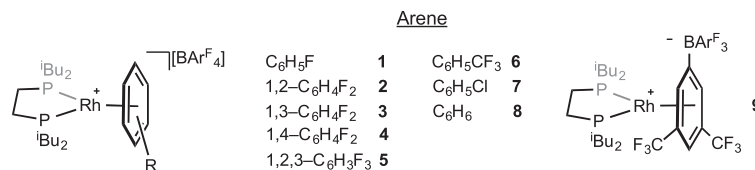
Synthesis and characterization of η^6 -arene complexes

We start by comparing the relative binding strengths of a variety of fluorinated arenes ligated with the $[\text{Rh}(\text{tBu}_2\text{PCH}_2\text{CH}_2\text{P}^i\text{Bu}_2)]^+$ fragment, a motif that we have previously used for the synthesis of a transition metal alkane complex in the solid-state [24]. Complexes **1**, $[\text{Rh}(\text{tBu}_2\text{PCH}_2\text{CH}_2\text{P}^i\text{Bu}_2)(\eta^6\text{-C}_6\text{H}_5\text{F})][\text{BAR}^{\text{F}}_4]$, and **2**, $[\text{Rh}(\text{tBu}_2\text{PCH}_2\text{CH}_2\text{P}^i\text{Bu}_2)(\eta^6\text{-1,2-C}_6\text{H}_4\text{F}_2)][\text{BAR}^{\text{F}}_4]$, have been reported as precursors as part of this study. Hydrogenation of $[\text{Rh}(\text{tBu}_2\text{PCH}_2\text{CH}_2\text{P}^i\text{Bu}_2)(\text{NBD})][\text{BAR}^{\text{F}}_4]$ (NBD = norbornadiene) in the presence of the desired arene (either as the solvent or as a reagent dissolved in non-coordinating CH_2Cl_2) results in the formation of the corresponding arene complex (Scheme 1). In most cases the resulting product can be recrystallized, after removal of the hydrogen atmosphere, by layering the reaction mixture directly with pentane to yield the products as analytically pure material. Using this methodology the following species were synthesized $[\text{Rh}(\text{tBu}_2\text{PCH}_2\text{CH}_2\text{P}^i\text{Bu}_2)(\eta^6\text{-arene})][\text{BAR}^{\text{F}}_4]$; arene = $\text{C}_6\text{H}_5\text{F}$ (**1**), 1,2- $\text{C}_6\text{H}_4\text{F}_2$ (**2**), 1,3- $\text{C}_6\text{H}_4\text{F}_2$ (**3**), 1,4- $\text{C}_6\text{H}_4\text{F}_2$ (**4**), 1,2,3- $\text{C}_6\text{H}_3\text{F}_3$ (**5**), $\text{C}_6\text{H}_5\text{CF}_3$ (**6**), $\text{C}_6\text{H}_5\text{Cl}$ (**7**), & C_6H_6 (**8**). Complexes **1**, **2** [24] and **7** [42] have been previously reported.

In solution all of the $[\text{Rh}(\text{tBu}_2\text{PCH}_2\text{CH}_2\text{P}^i\text{Bu}_2)(\eta^6\text{-arene})][\text{BAR}^{\text{F}}_4]$ complexes exhibited similar ^{31}P – ^{103}Rh coupling constants in their $^{31}\text{P}\{^1\text{H}\}$ NMR spectra ranging from 199 to 202 Hz, consistent with similar examples reported for $[\text{Rh}(\text{PR}_3)_2]^+$ fragments coordinated to arenes that generally show large (greater than 170 Hz) coupling constants [4,7,43]. The ^1H NMR spectra of the arene complexes in CD_2Cl_2 , or in the neat arene, show signals for the coordinated aromatics that are located upfield of signals for free ligand, indicative of η^6 -arene coordination [44]. In CD_2Cl_2 solvent these complexes are in equilibrium with the anion-coordinated zwitterionic complex **9** (vide infra) [24], and the ratio of these two species depends on the arene. No evidence of a κ_{F} -fluorine coordination mode is observed in solution by NMR spectroscopy (including ^{19}F NMR spectroscopy [17]). For many of these complexes the solid-state structures were determined, but unfortunately all show significant



Scheme 2. Various coordination modes of fluoro-arene ligands to metal centers.



Scheme 3. The range of arene complexes synthesized with the $\{Rh(iBu_2PCH_2CH_2P^iBu_2)\}^+$ fragment.

disorder in both the phosphine and the fluoroarene. Although they could be modelled satisfactorily to give gross structures fully consistent with an η -coordinated arene ligand, due to the high number of necessary restraints in refinement, imposed by the disorder, discussion of the structural metrics is not appropriate (see [Supporting materials](#)). Nevertheless the spectroscopic, and micro-analytical data, are in full accord with the proposed structures.

All these complexes show the molecular ion in the ESI–MS spectrum, when the appropriate fluoroarene solvent is used as diluent, that also displays the correct isotope pattern. However for the most weakly bound arene, complex **5**, at the required dilutions required for ESI–MS (1×10^{-6} mol dm $^{-3}$) [38] trace amounts of arene impurities present in the solvent, such as benzene and fluoroarene, displace a significant proportion of the weakly bound 1,2,3- $C_6H_3F_3$ ligand and so, although **5** is observed in the mass spectrum ($[M^+]$ $m/z = 553.19$, $[M^+]$ calc = 553.18, correct isotope pattern), it is only a minor peak (ca. 20%) with major peaks observed assigned to the cations of **1** and **8** [Scheme 3](#).

By contrast hydrogenation of $[Rh(iBu_2PCH_2CH_2P^iBu_2)(NBD)][BAR^F_4]$ in 1,2,3,4- $C_6H_2F_4$, C_6HF_5 or C_6F_6 solvents forms zwitterionic **9** as the sole product ([Scheme 4](#)) to the detection limits of ^{31}P NMR spectroscopy. In these cases the fluorobenzene now acts as a non-coordinating solvent.

Comparison of binding strength with the $[BAR^F_4]^-$ anion

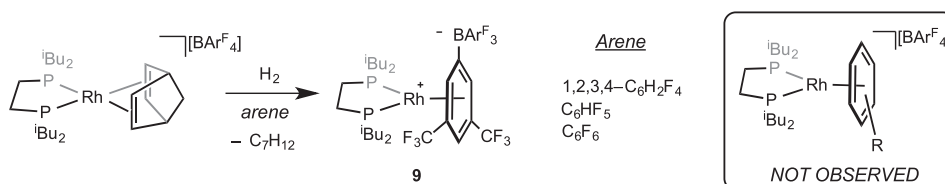
As the number of fluorine substituents on the arene is increased the $[BAR^F_4]^-$ anion thus becomes a competitive ligand for coordination, to form zwitterionic **9**, there being a tipping point in neat arene solvent with four fluorines in the arene. The position of the equilibrium between the arene complexes **1–8** and **9** can be measured using CH_2Cl_2 solutions and the relative integrals of each species in the $^{31}P\{^1H\}$ NMR spectrum, allowing for the equilibrium constant at 298 K to be estimated ([Table 1](#)). Although **9** undergoes decomposition in neat CH_2Cl_2 over 1 h, equilibrium is established rapidly allowing for measurements to be taken upon freshly solvated samples [45]. The corresponding reverse reaction, i.e. addition of C_6H_5F to **9** in CH_2Cl_2 solution, quickly formed complex **1**, demonstrating equilibrium conditions. These experiments show that by increasing the fluorine content of the arene the binding affinity of the arene with the $\{Rh(iBu_2PCH_2CH_2P^iBu_2)\}^+$ fragment decreases relative to $[BAR^F_4]^-$. The resulting $\Delta G_{(298\text{ K})}$ values obtained can be plotted against the number of fluorine substituents to show a reasonably linear trend [[Fig. 1](#)]. Noteworthy is that C_6H_6

(complex **8**) binds so strongly that complex **9** is not observed to the detection limits of ^{31}P NMR spectroscopy. As reported previously, complex **7** does not undergo C–Cl bond activation unlike the C_6H_5Br analogue (thus precluding equilibrium measurements for the bromoarene) [42]. Interestingly, $C_5H_6CF_3$ binds less strongly than the $[BAR^F_4]^-$ anion (which contains a bis- CF_3 substituted arene). We have previously reported that $[BAR^F_4]^-$ coordination with a $\{Rh(L)_2\}^+$ fragment is disfavoured entropically when compared with binding of $[CB_{11}H_6Br_6]^-$ [25]. However, in this example, the favourable electrostatic interactions in the zwitterion **9** are presumably also important in determining the position of equilibrium.

Estimation of relative binding affinities of the arene in $[Rh(iBu_2PCH_2CH_2P^iBu_2)(\eta^6\text{-arene})]^+$ using ESI–MS techniques

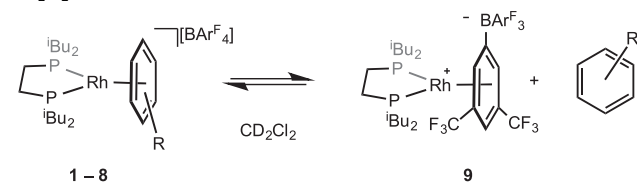
The phosphine complexes $[Rh(iBu_2PCH_2CH_2P^iBu_2)(\eta^6\text{-arene})]^+$ are ideal for gas-phase ESI–MS fragmentation studies because the phosphine is not susceptible to C–H activation, unlike monodentate iBu_3P complexes [46]. Controlled fragmentation experiments were achieved by use of a glove–box interfaced with an ESI–MS [38], and variation of the capillary exit voltage to determine the degree of fragmentation by collision–induced dissociation processes in the source [34]. By such variation, the ratio of the arene–coordinated cation, $[Rh(iBu_2PCH_2CH_2P^iBu_2)(\eta^6\text{-arene})]^+$, to the nominally 12–electron, arene–free, rhodium phosphine fragment $\{Rh(iBu_2PCH_2CH_2P^iBu_2)\}^+$ can be controlled. In the gas phase it is likely that this arene–free fragment is stabilized by agostic interactions from the alkyl phosphine [46–48], but as the same species is being formed in each case then the experiment probes just the relative binding strength of the arene. The results are plotted as the percentage of arene–bound cations against exit voltage in [Fig. 2](#) for selected species and tabulated for the full series in [Table 1](#).

In each experiment the corresponding arene complex was diluted to a concentration of $\sim 1 \times 10^{-6}$ M, using the same arene as the coordinated ligand as the solvent (to avoid formation of **9**), and the ESI–MS was recorded over a range of exit voltage values until less than 1% of the precursor ion remained. The spectra were analyzed by measuring the intensity of the largest isotope peak for the two signals $[Rh(iBu_2PCH_2CH_2P^iBu_2)(\eta^6\text{-arene})]^+$ and $[Rh(iBu_2PCH_2CH_2P^iBu_2)]^+$, and these intensities then normalized to account for differing isotopic distributions. Voltages were corrected to center-of-mass values with the assumption that the vast majority of collisions at this point in the source are with residual



Scheme 4. Hydrogenation (1 atm) of $[Rh(iBu_2PCH_2CH_2P^iBu_2)(NBD)][BAR^F_4]$ in fluorobenzenes $C_6H_{6-n}F_n$ ($n = 4–6$).

Table 1
Estimated equilibrium constants for arene complexes in equilibrium with **9** at 298 K in CH₂Cl₂.



Complex	Arene	$K(298)$	$\Delta G_{(298\text{ K})}$ (kJ mol ⁻¹)	Exit-voltage for 50% dissociation (V) ^b
8	C ₆ H ₆	$<1 \times 10^{-4}$	$>+25$ (min value)	8.4
1	C ₆ H ₅ F	$3 (\pm 1.4) \times 10^{-3}$	$+14 (\pm 1)$	7.2
2	1,2-F ₂ C ₆ H ₄	$3.2 (\pm 0.3)$	$-2.9 (\pm 0.2)$	6.3
3	1,3-F ₂ C ₆ H ₄	$12 (\pm 0.2)$	$-6.1^a (\pm 0.3)$	6.2
4	1,4-F ₂ C ₆ H ₄	$2.8 (\pm 0.3)$	$-2.5^a (\pm 0.2)$	6.4
5	1,2,3-F ₃ C ₆ H ₃	$260 (\pm 125)$	$-14 (\pm 1)$	3.9^c
6	C ₆ H ₅ CF ₃	$0.23 (\pm 0.22)$	$+3.6 (\pm 0.2)$	6.4
7	C ₆ H ₅ Cl	$6.1 (\pm 6.4) \times 10^{-4}$	$+18 (\pm 3)$	7.1

^a Estimated value as ~15% of **1** present from impurities in the solvent (Fluorochem).

^b Exit-voltage at which 50% arene dissociation occurs from ESI-MS (mass corrected).

^c This species is present at small relative concentrations in the gas-phase due to the competitive formation of alternate cations such as **1** and **8** that arise from trace solvent impurities.

dinitrogen desolvation gas [34]. The point at which 50% fragmentation occurs was taken as a suitable and convenient value for comparison. The fragmentation profiles, shown in Fig. 2 and tabulated in Table 1, clearly show that as extra fluorine substituents are added to the arene the binding affinity of the arene drops, consistent with previous reports and calculations [30,49–52]. The fragmentation profile of **5**, whilst broadly the same line-shape as for the other complexes, is distorted due to a large signal for the fragmented species $[\text{Rh}(\text{iBu}_2\text{PCH}_2\text{CH}_2\text{P}^i\text{Bu}_2)]^+$, even at low exit-voltages. We suggest that this could be because the signal for $[\text{Rh}(\text{iBu}_2\text{PCH}_2\text{CH}_2\text{P}^i\text{Bu}_2)(\eta^6\text{-1,2,3-F}_3\text{C}_6\text{H}_3)]^+$ represents a minor proportion (ca. 20%) of the mixture compared with species that contribute to the $[\text{Rh}(\text{iBu}_2\text{PCH}_2\text{CH}_2\text{P}^i\text{Bu}_2)]^+$ peak arising from more strongly binding impurities in the 1,2,3-C₆H₃F₃ solvent, such as **1** and **8**. Even at low exit voltages a small but significant fragmentation of these species is occurring, and under the conditions of

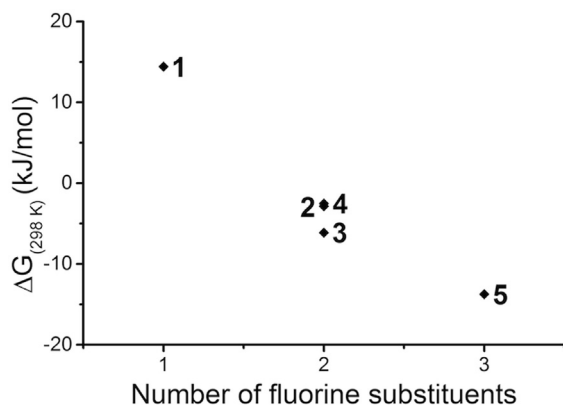


Fig. 1. Plot of $\Delta G_{(298\text{ K})}$ versus degree of fluorine substitution for the equilibrium $(\mathbf{1-5}) \rightleftharpoons \mathbf{9}$.

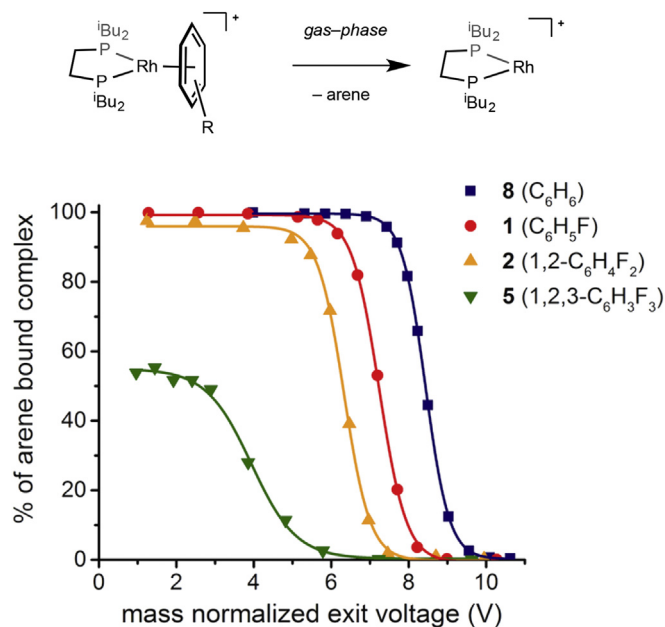


Fig. 2. Selected plots of fragmentation of $[\text{Rh}(\text{iBu}_2\text{PCH}_2\text{CH}_2\text{P}^i\text{Bu}_2)(\eta^6\text{-C}_6\text{H}_{6-n}\text{F}_n)]^+$ ($n = 0-3$) cations in ESI-MS over a range of exit-voltage values.

high dilution this results in a significant amount of $[\text{Rh}(\text{iBu}_2\text{PCH}_2\text{CH}_2\text{P}^i\text{Bu}_2)]^+$ to be observed. Alternatively we suggest the formation of neutral zwitterionic **9** in the gas phase with this particularly weakly binding solvent, from which fragmentation to form $[\text{Rh}(\text{iBu}_2\text{PCH}_2\text{CH}_2\text{P}^i\text{Bu}_2)]^+$ would account for its observation at low exit-voltages. Although the measurement of **5** is thus rather qualitative, the profile of 50% fragmentation from the measured maximum decreases in magnitude with increasing fluorine incorporation is consistent, and correlates with, with the $K(298)$ values measured in CH₂Cl₂. Thus we suggest that these variable exit voltage ESI-MS experiments offer a good qualitative methodology for assessing the strength of arene binding in $[\text{Rh}(\text{iBu}_2\text{PCH}_2\text{CH}_2\text{P}^i\text{Bu}_2)(\eta^6\text{-C}_6\text{H}_{6-n}\text{F}_n)]^+$ complexes.

In Fig. 3 the three isomeric difluorobenzene complexes **2**, **3** and **4** show very similar 50% fragmentation points [as well as $K(298)$, Table 1] suggesting substituent positioning is not very influential on the overall binding affinity of these arenes. By contrast, in rhenium η^2 -fluorobenzene complexes, $\text{Re}(\eta\text{-C}_5\text{H}_5)(\text{CO})_2(\text{C}_6\text{H}_{6-x}\text{F}_x)$

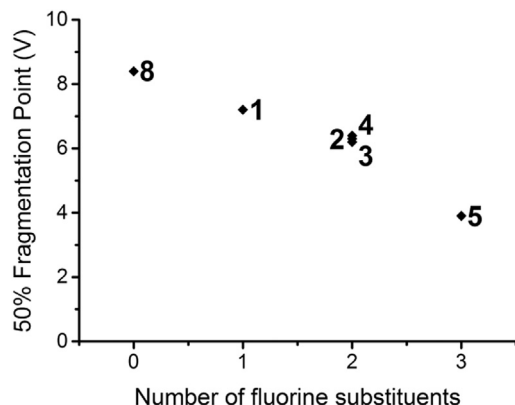


Fig. 3. Comparison of the mass normalized 50% fragmentation point of $[\text{Rh}(\text{iBu}_2\text{PCH}_2\text{CH}_2\text{P}^i\text{Bu}_2)(\eta^6\text{-C}_6\text{H}_{6-n}\text{F}_n)]^+$ with number of fluorine substituents (n).

($x = 0-5$), the binding affinities are highly dependent upon fluorine position, as coordination to the HC=CH unit of the arene is favoured over FC=CH, so that 1,2,3- $C_6H_3F_3$ binds more strongly than 1,3,5- $C_6H_3F_3$ for example [21].

Estimation of binding affinities of $[Rh(L_2)(\eta^6-C_6H_5F)][BAR^F_4]$ complexes ($L_2 =$ chelating phosphine) using ESI-MS techniques

Having established that variation of exit voltage in ESI-MS offers a qualitative measure of the strength of arene binding we then moved to probe the effect of phosphine ligand while keeping the arene fixed (C_6H_5F). The effect of phosphine substituent sterics/electronic profile [53], and chelate bite angle [27,28] was probed by using a range of rhodium $\eta^6-C_6H_5F$ complexes. Scheme 5 presents the complexes studied. Many of these complexes have been previously reported, for example in hydroacylation [3,4] and C-S bond cleavage catalysis [6]. The complex $[Rh(\{^iPrO\}_2PCH_2CH_2P\{O^iPr\}_2)(\eta^6-C_6H_5F)][BAR^F_4]$, **16**, is new and was prepared by hydrogenation of the NBD precursor. The solid-state structure of complex **16** is presented in Fig. 4, and the structural metrics are unremarkable.

Table 2 and Figs. 5 and 6 present the data collected, which show some interesting trends. Firstly when comparing the bite-angle of the chelating phosphine while keeping the P-functionality the same (i.e. P^iPr_2) there is a clear trend for those ligands with methylene spacers that increasing the bite angle leads to a more labile arene ligand (**12** < **15** < **17**, Fig. 5). Whether this is a result of decreased Rh-arene bond strength or increased stability in the gas phase of the $\{Rh(L_2)\}^+$ fragment (possibility stabilized by agostic interactions) is currently not clear, although we have noted a similar trend in this series of complexes when dissolved in acetone solvent, in that the wider bite angle-ligands promote for equilibrium mixtures that favor the acetone adducts, i.e. $[Rh(L_2)(acetone)_2][BAR^F_4]$ [4]. Such bis-adducts are unlikely to have significant agostic interactions. We have also previously noted that wider-bite angle $\{Rh(L_2)\}^+$ fragments promote stronger binding with amine-boranes through Rh-H-B interactions [7,8], and qualitatively explained this by a better match between the frontier orbitals of the metal fragment with the B-H bonds on increasing bite angle [8]. Complex **11** lies a little below that of **12**, even though the ligand has a smaller bite angle. This might reflect the electronic influence of the NMe over the CH_2 group, in which delocalization of the nitrogen lone pair over the chelate has suggested to be significant in the improved performance of these ligands in ethene oligomerization catalysis. [55,56]

Comparison of differing phosphine functionalities while keeping the bite angle similar is also instructive, and this is facilitated by the range of small-bite angle methylene-backbone PCP-type ligands [57] that can be synthesized with tBu , Cy and iPr substituents (Fig. 6, Table 2). Interrogation of these species using variable exit-voltage ESI-MS shows that the order of ease of dissociation of the fluorobenzene ligand increases in the order tBu

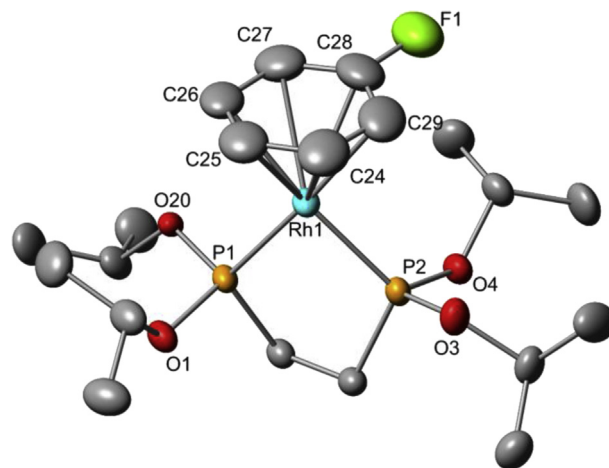


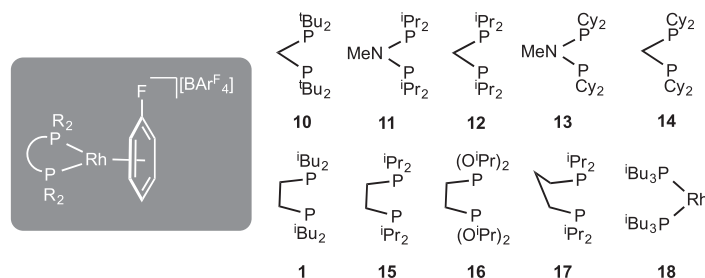
Fig. 4. Displacement ellipsoid plot (30% probability) of complex **16** in the solid state. Major disorder component shown only. Hydrogen atoms and anion omitted for clarity. Selected bond length (Å) and angle ($^\circ$) data. Rh-C_{aryl} max/min: Rh(1)-C(28), 2.345(6)/Rh(1)-C(26), 2.297(5); Rh(1)-P(1), 2.2042(12); Rh(1)-P(2), 2.2091(12); P(1)-Rh(1)-P(2), 82.83(4).

(**10**) < iPr (**12**) < Cy (**14**) while the bite angles remain similar. This is counter-intuitive to the expected trend from simple steric arguments that would predict the bulky tBu -substituted phosphine to have the most labile fluoroarene ligand. The trend might, instead, reflect the ability for the $[Rh(L_2)]^+$ fragment to form stabilizing agostic bonds in the gas phase. This is perhaps demonstrated by that the fluoroarene complex **18** cannot be observed in the gas phase, even at very low exit voltages, with only the $[Rh(P^iBu_3)_2]^+$ fragment observed. It is likely that the lack of chelate backbone allows for more efficient agostic interactions from the phosphine, as we have shown for example, in the crystallographically-characterized $[Rh(P^iBu_3)_2(H)_2][BAR^F_4]$ [54], and suggested to occur in $[Rh(P^iBu_3)_2][BAR^F_4]$. By contrast, comparison of the quasi-isosteric phosphine complexes **1** (P^iBu_2) and **16** ($P(O^iPr)_2$) which have ethylene backbones show that the arene is lost more readily in the former, suggesting stronger arene binding with the phosphite.

Comparisons with ESI-MS/MS data

In order to test the reliability of the variable exit-voltage ESI-MS technique a selection of the fluorobenzene compounds were screened using ESI-MS/MS techniques, where the fragmentation of a selected mass species is controlled by altering the voltage across an argon-filled collision cell [33,34].

Fig. 7 shows these data, which when plotting the resulting 50% fragmentation voltages from these collision cell CID experiments against the in-source CID values shows a good, almost linear,



Scheme 5. Range of C_6H_5F complexes synthesized with the $\{Rh(L_2)\}^+$ fragments.

Table 2
Exit-voltage at which 50% arene dissociation occurs (in order of decreasing voltage).

Complex	Backbone length, P–Rh–P (°)	P–Substituents	Exit-voltage for 50% dissociation (V) ^a
10	1, 74.57(5) [3]	^t Bu	11.1
12	1, 72.64(5) [4]	ⁱ Pr	10.5
11	1 (N), 70.36(3) [4]	ⁱ Pr	10.4
15	2, 84.81(3) [4]	ⁱ Pr	9.7
13	1 (N), 70.49(4) [4]	Cy	8.8
14	1, 72.78(3) [3]	Cy	8.7
16	2, 82.83(4)	O ⁱ Pr	8.1
17	3, 93.78(3) [4]	ⁱ Pr	8.1
1	2, 84.21(6) ^b [24]	ⁱ Bu	7.2
18	n/a, 95.31(5)[54]	ⁱ Bu	<1.8

^a Mass Corrected.

^b Reported as the NBD adduct.

correlation (Fig. 8), thus demonstrating the validity of both approaches to produce a qualitative ordering.

The effect that steric factors have on the strength of binding can also be probed easily by the simple expedient of adding a drop of a more strongly binding arene (e.g. a non-fluorinated one) to a fluoro-benzene solution of $[\text{Rh}(\text{}^i\text{Pr}_2\text{PNMeP}^i\text{Pr}_2)(\text{C}_6\text{H}_5\text{F})][\text{BAR}^{\text{F}}_4]$, **11**. This experiment was conducted for the arenes benzene, toluene, xylene and mesitylene (Fig. 9). The arene complex formed was probed by ESI–MS in each case, and the new complex was selected for CID and fragmented progressively in the collision cell using Ar. These data

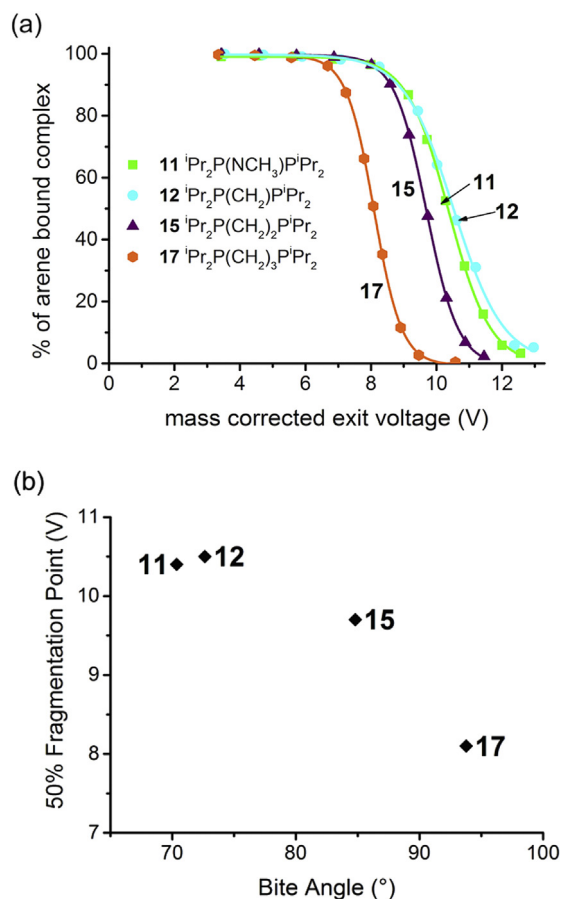


Fig. 5. (a) Plots of fragmentation of $[\text{Rh}(\text{L}_2)(\eta^6\text{-FC}_6\text{H}_5)]^+$ cations in ESI–MS over a range of exit voltage values. (b) Comparison of 50% fragmentation point of $[\text{Rh}(\text{L}_2)(\eta^6\text{-C}_6\text{H}_5\text{F})]^+$ for the ⁱPr–substituted phosphines. See Scheme 5 for labelling.

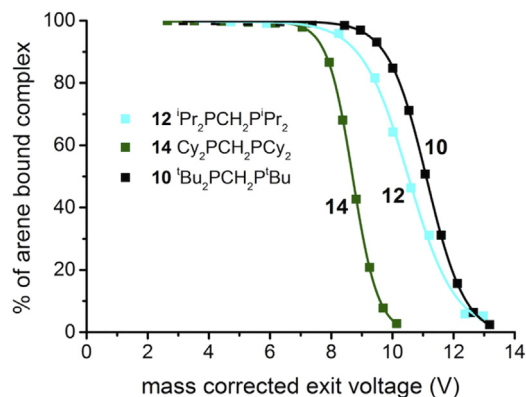


Fig. 6. Fragmentation of $[\text{Rh}(\text{R}_2\text{PCH}_2\text{PR}_2)(\eta^6\text{-C}_6\text{H}_5\text{F})]^+$ ($\text{R} = \text{}^i\text{Pr}, \text{Cy}$ or ^tBu) cations in ESI–MS over a range of exit voltage values.

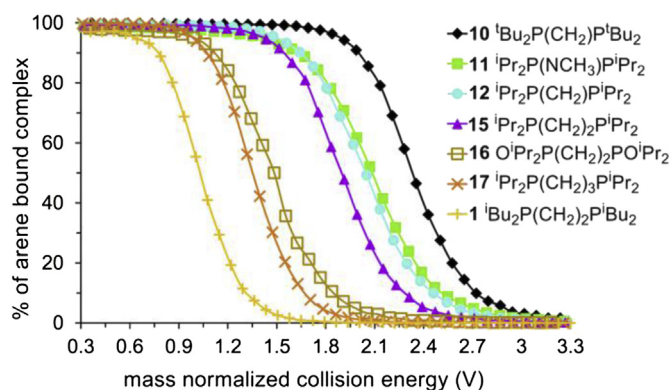


Fig. 7. CID data from MS/MS experiments on **10**, **11**, **12**, **15**, **16**, **17** and **1**. Collision energy has been normalized to center of mass.

show that the fluoro-benzene complex is substantially easier to fragment using CID than any of the hydrocarbon-only arenes. While all four complexes $[\text{Rh}(\text{}^i\text{Pr}_2\text{PNMeP}^i\text{Pr}_2)(\text{C}_6\text{H}_{6-n}\text{Me}_n)]^+$ ($n = 0\text{--}3$) all dissociate their arene at about the same collision energy, there is a discernible trend towards it being more difficult to dissociate the more electron-rich arenes, despite steric effects acting to weaken the strength of the metal–ligand bonding.

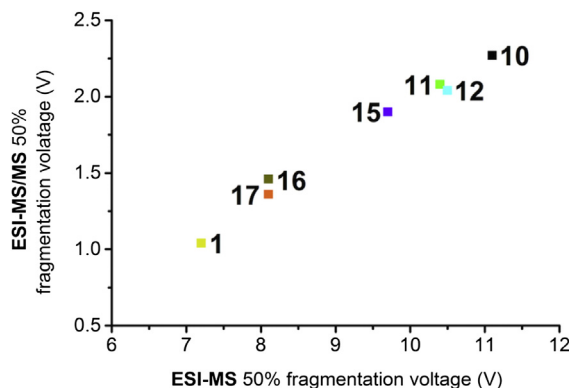


Fig. 8. Correlation between ESI–MS experiments and ESI–MS/MS experiments (mass corrected).

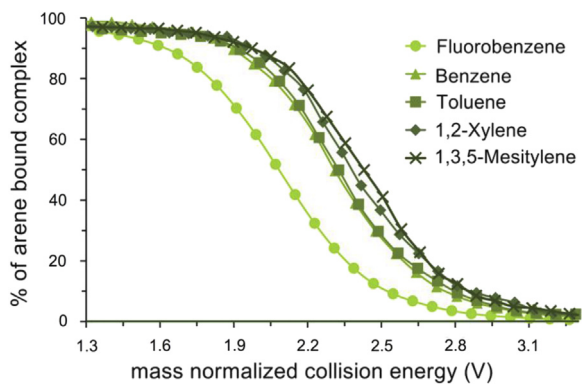


Fig. 9. Comparison of the 50% fragmentation point of $[\text{Rh}(\text{L})(\eta^6\text{-C}_6\text{H}_5\text{F})]^+$, L = benzene, toluene, xylene and mesitylene, and compared with that for complex **11** (fluorobenzene).

Conclusions

A collection of CID experiments have been undertaken which probe the relative dissociation energy of an arene from a variety of η^6 -arene complexes of the type $[\text{Rh}(\text{L}_2)(\eta^6\text{-arene})][\text{BAR}^{\text{F}}_4]$. These experiments show that increasing the number of electron withdrawing substituents reduces the binding affinity of the arene. The ordering of these results are in agreement with equilibrium measurements in CD_2Cl_2 solution, in which the $[\text{BAR}^{\text{F}}_4]^-$ anion can displace the coordinated arene. The gas-phase binding affinity of $\text{C}_6\text{H}_5\text{F}$ is also much greater in conjunction with smaller bite angle phosphine ligands, or with more electron withdrawing phosphites. The phosphine substituents also influence the gas-phase binding affinity of $\eta^6\text{-C}_6\text{H}_5\text{F}$, with ^tBu groups associated with the greatest binding affinities and cyclohexyl groups with the least, of those tested. Overall it is likely that these trends reflect a combination of arene binding strength and stabilization of the low-coordinate $\{\text{Rh}(\text{L}_2)\}^+$ fragment in the gas-phase and computational studies are currently underway to delineate these factors.

These simple in-source and collision cell CID experiments can be performed quickly and without any extra modifications using standard ESI-MS(/MS) instruments, and are thus potentially useful processes for the qualitative comparison of the relative stabilities of various organometallic complexes.

Experimental section

General details

All manipulations, unless otherwise stated, were performed under an atmosphere of argon, using standard Schlenk-line and glovebox techniques. Glassware was oven-dried at 403 K overnight and flamed under vacuum prior to use. CH_2Cl_2 , pentane and hexane were dried using a Grubbs-type solvent purification system (MBraun SPS-800) and degassed by successive freeze-pump-thaw cycles [58]. CD_2Cl_2 , and all fluorobenzene and trifluorotoluene solvents, were distilled under vacuum from CaH_2 and stored over 3 Å molecular sieves (difluorobenzenes were also stirred over alumina prior to distillation). $\text{Na}[\text{BAR}^{\text{F}}_4]$ [59], $(\text{O}^i\text{Pr})_2\text{PCH}_2\text{CH}_2\text{-P}(\text{O}^i\text{Pr})_2$ [60,61], $[(\text{NBD})\text{RhCl}_2]$ [62] and $[\text{Rh}(^i\text{Bu}_2\text{PCH}_2\text{CH}_2\text{P}^i\text{Bu}_2)(\text{NBD})][\text{BAR}^{\text{F}}_4]$ [24], were prepared by the literature procedures. Complexes **1** [24], **2** [24], **7**, [42] **10** [3], **11** [4], **12** [4], **13** [4], **14** [4], **15** [4], **17** [4], **18** [54] have been described previously. All other reagents were used as received from suppliers. NMR spectra were recorded on Varian Unity 500 MHz, Bruker AVD 500 MHz, or Varian

Mercury 300 MHz spectrometers at room temperature unless otherwise stated. Non-Deuterated Solvents were locked to a standard C_6D_6 solution. Residual protio solvent was used as reference for ^1H , ^2H and ^{13}C NMR spectra in deuterated solvent samples. In $1,2\text{-C}_6\text{H}_4\text{F}_2$ and $\text{C}_6\text{H}_5\text{F}$ ^1H NMR spectra were referenced to the centre of the downfield solvent multiplet (δ 7.07 and δ 7.11 respectively). ^{31}P NMR spectra were externally referenced to 85% H_3PO_4 . All chemical shifts (δ) are quoted in ppm and coupling constants in Hz. Elemental micro-analysis carried out upon crystalline samples dried under dynamic vacuum (1×10^{-2} Torr) overnight, by Stephen Boyer at London Metropolitan University.

Electrospray Ionisation Mass Spectrometry (ESI-MS) experiments were recorded using a Bruker MicrOTOF instrument directly connected to a modified Innovative Technology glovebox [38]. Typical acquisition parameters were as follows: sample flow rate [4 $\mu\text{L}/\text{min}$], nebuliser gas pressure [0.4 bar], drying gas [argon at 333 K, flowing at 4 L/min], capillary voltage [4.5 kV], exit voltage [60 V (variable exit voltage studies 20–250 V)]. The spectrometer was calibrated using a mixture of tetralkyl ammonium bromides $[\text{N}(\text{C}_n\text{H}_{2n+1})_4]\text{Br}$ ($n = 2\text{--}8, 12, 16$ & 18). Samples were diluted to a concentration of 1×10^{-6} M in the appropriate solvent before running. Variable exit-voltage experiments were measured for ~ 10 s per voltage step, and the intensity of the largest isotope peak of the fragmented and non-fragmented signals were recorded. Subsequently the intensities were normalized to account for the varying isotopic distributions. In arene dissociation experiments where multiple fragmentation products were formed (see Supporting materials) the intensities of the fragmented products were summed and compared to the non-fragmented intensity. None of the secondary fragments coordinate arene ligands and so are presumed to form after initial arene dissociation. ESI-MS/MS experiments were recorded using a Micromass Q-ToF micro instrument in positive ion mode using pneumatically assisted electrospray ionization. Typical experimental parameters were: capillary voltage, 2900 V; sample cone voltage, 15 V; extraction voltage, 0.5 V; source temperature, 84 °C; desolvation temperature, 184 °C; cone gas flow, 100 L/h; desolvation gas flow, 200 L/h; MCP voltage, 2400 V. Samples were prepared by dilution in fluorobenzene to a concentration of 0.15 mM and introduced into the source at 10 ml/min via a syringe pump. Data collection was carried out in continuum mode and spectra were collected by selecting the parent ion of interest by the quadrupole. A scan time of 5 s per spectrum was used. The collision cell voltage was set to 0 V initially and increased by increments of 1 V per scan, up to a maximum of 60 V. Resultant data was corrected to the centre of mass according to the formula

$$E_0 = E_{\text{lab}} * m_A / (m_A + m_1)$$

where E_{lab} is the collision cell voltage, m_A is the mass of the collision gas and m_1 is the mass of the target ion.

New complexes

$[\text{Rh}(^i\text{Bu}_2\text{PCH}_2\text{CH}_2\text{P}^i\text{Bu}_2)(\eta^6\text{-1,3-C}_6\text{H}_4\text{F}_2)][\text{BAR}^{\text{F}}_4]$ (**3**)

18 mg (0.013 mmol) of $[\text{Rh}(^i\text{Bu}_2\text{PCH}_2\text{CH}_2\text{P}^i\text{Bu}_2)(\text{NBD})][\text{BAR}^{\text{F}}_4]$ was dissolved in $1,3\text{-C}_6\text{H}_4\text{F}_2$ in a high pressure NMR tube. The tube was charged with 1 atm H_2 . A yellow solution of **3** forms upon shaking. The hydrogen gas was removed and pentane added to crystallise the product directly from the solution (Yield 9 mg, 49%). ^1H NMR (500 MHz $1,3\text{-C}_6\text{H}_4\text{F}_2$ ref upfield solvent signal δ 7.16): δ 1.03 (d (^iBu CH₃), $J_{\text{HH}} = 6$ Hz, 12H), 1.11 (d (^iBu CH₃), $J_{\text{HH}} = 6$ Hz, 12H), 1.66 (m (^iBu CH₂), 8H), 1.78 (d (PCH₂CH₂P), $J_{\text{PH}} = 17$ Hz, 4H), 1.88 (m (^iBu CH), 4H), 6.07 (s (1,3- $\text{C}_6\text{H}_4\text{F}_2$), 2H), 7.68 (s (BAR^{F}_4), 4H), 8.28 (s (BAR^{F}_4), 8H). Two aryl protons unaccounted for, likely to be

observed by the solvent. ^1H NMR (500 MHz CD_2Cl_2): {N.B. minor species (~20%) in CD_2Cl_2 solution as is in equilibrium with **9**. δ 1.03 (d (^iBu CH_3), $J_{\text{HH}} = 7$ Hz, 12H), 1.09 (d (^iBu CH_3), $J_{\text{HH}} = 7$ Hz, 12H), 1.2–1.9 (m ($\text{PCH}_2\text{CH}_2\text{P}$, ^iBu CH & $^i\text{Bu}_2$), 16H), 6.19 (m (1,3- $\text{C}_6\text{H}_4\text{F}_2$), 2H), 7.01 (m (1,3- $\text{C}_6\text{H}_4\text{F}_2$), H), 7.56 (s (BAR^{F_4}), 4H), 7.72 (s (BAR^{F_4}), 8H). One arene resonance not located, it is likely coincident with another signal. $^{31}\text{P}\{^1\text{H}\}$ NMR (202 MHz 1,3- $\text{C}_6\text{H}_4\text{F}_2$): δ 72.8 (d, $J_{\text{RHP}} = 200$ Hz, 2P). $^{19}\text{F}\{^1\text{H}\}$ NMR (169 MHz 1,3- $\text{C}_6\text{H}_4\text{F}_2$): δ -123.4 (s (1,4- $\text{C}_6\text{H}_4\text{F}_2$), 2F), -62.9 (s (BAR^{F_4}), 24F). ESI-MS: $[\text{M}^+]$ $m/z = 535.19$, $[\text{M}^+]$ calc = 535.19 (correct isotope pattern). Elemental Micro-Analysis: $\text{C}_{56}\text{H}_{56}\text{BF}_{26}\text{P}_2\text{Rh}$ C, 47.97H, 3.84 found C, 48.09H, 4.04.

$[\text{Rh}(^i\text{Bu}_2\text{PCH}_2\text{CH}_2\text{P}^i\text{Bu}_2)(\eta^6\text{-}1,4\text{-C}_6\text{H}_4\text{F}_2)][\text{BAR}^{\text{F}_4}]$ (**4**)

16 mg (0.012 mmol) of $[\text{Rh}(^i\text{Bu}_2\text{PCH}_2\text{CH}_2\text{P}^i\text{Bu}_2)(\text{NBD})][\text{BAR}^{\text{F}_4}]$ was dissolved in CH_2Cl_2 (0.4 ml) in a high pressure NMR tube and 0.1 ml of 1,4- $\text{C}_6\text{H}_4\text{F}_2$ was added. The tube was charged with 1 atm H_2 and a yellow solution of **4** forms upon shaking. The hydrogen gas was removed and pentane added to crystallise the product directly from the solution (Yield = 11 mg, 68%). **4** is not soluble in neat 1,4- $\text{C}_6\text{H}_4\text{F}_2$. ^1H NMR (500 MHz CD_2Cl_2): {N.B. minor species (~20%) in CD_2Cl_2 solution as is in equilibrium with **9**. δ 1.02 (d (^iBu CH_3), $J_{\text{HH}} = 7$ Hz, 12H), 1.09 (d (^iBu CH_3), $J_{\text{HH}} = 7$ Hz, 12H), 1.2–1.9 (m ($\text{PCH}_2\text{CH}_2\text{P}$, ^iBu CH & $^i\text{Bu}_2$), 16H), 6.81 (t (1,4- $\text{C}_6\text{H}_4\text{F}_2$), $J_{\text{FH}} = 3$ Hz, 4H), 7.56 (s (BAR^{F_4}), 4H), 7.72 (s (BAR^{F_4}), 8H). $^{31}\text{P}\{^1\text{H}\}$ NMR (202 MHz CD_2Cl_2): δ 73.2 (d, $J_{\text{RHP}} = 200$ Hz). $^{19}\text{F}\{^1\text{H}\}$ NMR (169 MHz CD_2Cl_2): δ -132.2 (s (1,4- $\text{C}_6\text{H}_4\text{F}_2$), 2F), -62.87 (s (BAR^{F_4}), 24F). ESI-MS: $[\text{M}^+]$ $m/z = 535.19$, $[\text{M}^+]$ calc = 535.19 (correct isotope pattern). Elemental Micro-Analysis: $\text{C}_{56}\text{H}_{56}\text{BF}_{26}\text{P}_2\text{Rh}$ C, 48.09; H, 4.04 found C, 48.27; H, 3.94.

$[\text{Rh}(^i\text{Bu}_2\text{PCH}_2\text{CH}_2\text{P}^i\text{Bu}_2)(\eta^6\text{-}1,2,3\text{-C}_6\text{H}_3\text{F}_3)][\text{BAR}^{\text{F}_4}]$ (**5**)

8 mg (0.006 mmol) of $[\text{Rh}(^i\text{Bu}_2\text{PCH}_2\text{CH}_2\text{P}^i\text{Bu}_2)(\text{NBD})][\text{BAR}^{\text{F}_4}]$ was dissolved in 1,2,3- $\text{C}_6\text{H}_3\text{F}_3$ in a high pressure NMR tube. The tube was charged with 1 atm H_2 . A yellow solution of **5** forms upon shaking. The complex was characterised in solution only. ^1H NMR (500 MHz 1,2,3- $\text{C}_6\text{H}_3\text{F}_3$ (referenced to left central peak of solvent quartet at δ 6.80)): δ 0.95 (d (^iBu CH_3), $J_{\text{HH}} = 7$ Hz, 12H), 1.03 (d (^iBu CH_3), $J_{\text{HH}} = 7$ Hz, 12H), 1.72 (m (^iBu CH_2), 8H), 1.88 (m ($\text{PCH}_2\text{CH}_2\text{P}$ and ^iBu CH), 8H), 7.37 (s (BAR^{F_4}), 4H), 7.97 (s (BAR^{F_4}), 8H). The ^1H NMR resonances of the bound 1,2,3- $\text{C}_6\text{H}_3\text{F}_3$ are likely to be obscured by the free solvent resonances. $^{31}\text{P}\{^1\text{H}\}$ NMR (202 MHz 1,2,3- $\text{C}_6\text{H}_3\text{F}_3$): δ 75.05 (d, $J_{\text{RHP}} = 203$ Hz, 2P). $^{19}\text{F}\{^1\text{H}\}$ NMR (282 MHz 1,2,3- $\text{C}_6\text{H}_3\text{F}_3$): δ -167.95 (t ($\text{C}_6\text{H}_3\text{F}_3$), $J_{\text{FF}} = 30$ Hz, F), -147.52 (d ($\text{C}_6\text{H}_3\text{F}_3$), $J_{\text{FF}} = 30$ Hz, 2F), -64.09 (s (BAR^{F_4}), 24F). ESI-MS: $[\text{M}^+]$ $m/z = 553.19$, $[\text{M}^+]$ calc = 553.18 (correct isotope pattern). No crystalline material suitable for micro-analysis was obtained.

$[\text{Rh}(^i\text{Bu}_2\text{PCH}_2\text{CH}_2\text{P}^i\text{Bu}_2)(\eta^6\text{-C}_6\text{H}_5\text{CF}_3)][\text{BAR}^{\text{F}_4}]$ (**6**)

11 mg (0.008 mmol) of $[\text{Rh}(^i\text{Bu}_2\text{PCH}_2\text{CH}_2\text{P}^i\text{Bu}_2)(\text{NBD})][\text{BAR}^{\text{F}_4}]$ was dissolved in $\text{C}_6\text{H}_5\text{CF}_3$ in a high pressure NMR tube. The tube was charged with 1 atm H_2 . A yellow solution of **6** forms upon shaking. The hydrogen was removed and pentane added to crystallise the product directly from the solution (Yield 8 mg, 70%). NMR Spectroscopy: ^1H NMR (300 MHz CD_2Cl_2): {N.B. major species (66%) in CD_2Cl_2 solution as is in equilibrium with **9**. δ 1.02 (d (^iBu CH_3), $J_{\text{HH}} = 7$ Hz, 12H), 1.08 (d (^iBu CH_3), $J_{\text{HH}} = 7$ Hz, 12H), 1.6–1.9 (m ($\text{PCH}_2\text{CH}_2\text{P}$, ^iBu CH & ^iBu CH_2), 16H), 6.46 (t ($\text{C}_6\text{H}_5\text{CF}_3$), $J_{\text{HH}} = 6$ Hz, 2H), 6.64 (d ($\text{C}_6\text{H}_5\text{CF}_3$), $J_{\text{HH}} = 6$ Hz, 2H), 6.94 (t ($\text{C}_6\text{H}_5\text{CF}_3$), $J_{\text{HH}} = 6$ Hz, 1H), 7.56 (s (BAR^{F_4}), 4H), 7.72 (s (BAR^{F_4}), 8H). $^{31}\text{P}\{^1\text{H}\}$ NMR (121 MHz CD_2Cl_2): δ 72.09 (d, $J_{\text{RHP}} = 200$ Hz, 2P). $^{19}\text{F}\{^1\text{H}\}$ NMR (282 MHz CD_2Cl_2): δ -61.36 or -61.01* (s ($\text{C}_6\text{H}_5\text{CF}_3$), 3F), -62.84 (s (BAR^{F_4}), 24F) *ambiguous to which peak is **6** and which is from **9**. ESI-MS: $[\text{M}^+]$ $m/z = 567.21$, $[\text{M}^+]$ calc = 567.20 (correct isotope pattern).

Elemental Micro-Analysis: $\text{C}_{57}\text{H}_{57}\text{BF}_{27}\text{P}_2\text{Rh}$ C, 47.85H, 4.02 found C, 47.90H, 3.95.

$[\text{Rh}(^i\text{Bu}_2\text{PCH}_2\text{CH}_2\text{P}^i\text{Bu}_2)(\eta^6\text{-C}_6\text{H}_6)][\text{BAR}^{\text{F}_4}]$ (**8**)

15 mg (0.011 mmol) of $[\text{Rh}(^i\text{Bu}_2\text{PCH}_2\text{CH}_2\text{P}^i\text{Bu}_2)(\text{NBD})][\text{BAR}^{\text{F}_4}]$ was dissolved in CH_2Cl_2 (0.4 ml) in a high pressure NMR tube and 0.05 ml of benzene was added. The tube was charged with 1 atm H_2 and left for 24 h. A yellow solution of **8** forms. The hydrogen gas was removed and pentane added to crystallise the product directly from the solution (Yield: 8 mg, 54%). ^1H NMR (500 MHz CD_2Cl_2): δ 1.00 (d (^iBu CH_3), $J_{\text{HH}} = 7$ Hz, 12H), 1.07 (d (^iBu CH_3), $J_{\text{HH}} = 7$ Hz, 12H), 1.63 (m (^iBu CH_2), 8H), 1.73 (d ($\text{PCH}_2\text{CH}_2\text{P}$), $J_{\text{PH}} = 17$ Hz, 4H), 1.85 (m (^iBu CH), 4H), 6.47 (s (C_6H_6), 6H), 7.56 (s (BAR^{F_4}), 4H), 7.72 (s (BAR^{F_4}), 8H). $^{31}\text{P}\{^1\text{H}\}$ NMR (202 MHz CD_2Cl_2): δ 73.4 (d, $J_{\text{RHP}} = 201$ Hz). ESI-MS: $[\text{M}^+]$ $m/z = 499.23$, $[\text{M}^+]$ calc = 499.21 (correct isotope pattern). Elemental Micro-Analysis: $\text{C}_{56}\text{H}_{58}\text{BF}_{24}\text{P}_2\text{Rh}$ C, 49.36H, 4.29 found C, 49.44H, 4.44.

$[\text{Rh}\{(\text{O}^i\text{Pr}_2)\text{PCH}_2\text{CH}_2\text{P}(\text{O}^i\text{Pr}_2)\}(\eta^6\text{-C}_6\text{H}_5\text{F})][\text{BAR}^{\text{F}_4}]$ (**16**)

25 mg (0.018 mmol) $[\text{Rh}\{(\text{O}^i\text{Pr}_2)\text{PCH}_2\text{CH}_2\text{P}(\text{O}^i\text{Pr}_2)\}(\text{NBD})][\text{BAR}^{\text{F}_4}]$ (below) was dissolved in $\text{C}_6\text{H}_5\text{F}$ in a high pressure NMR tube. The tube was charged with 1 atm H_2 . A pale yellow solution of **16** forms upon shaking. After 2.5 h the hydrogen was removed and pentane added to crystallise the product directly from the solution (Yield = 8 mg, 32%). ^1H NMR (500 MHz $\text{C}_6\text{H}_5\text{F}$): δ 1.13 (d (^iPr CH_3), $J_{\text{HH}} = 4$ Hz, 12H), 1.14 (d (^iPr CH_3), $J_{\text{HH}} = 4$ Hz, 12H), 1.55 (d ($\text{PCH}_2\text{CH}_2\text{P}$), $J_{\text{PH}} = 24$ Hz, 4H), 4.25 (m (OCHMe_2), 4H), 5.78 (t ($\text{C}_6\text{H}_5\text{F}$), $J_{\text{HH}} = 6$ Hz, ^1H), 6.29 (m ($\text{C}_6\text{H}_5\text{F}$), 2H), 6.36 (t ($\text{C}_6\text{H}_5\text{F}$), $J_{\text{HH}} = 6$ Hz, 2H), 7.66 (s (BAR^{F_4}), 4H), 8.33 (s (BAR^{F_4}), 8H). $^{31}\text{P}\{^1\text{H}\}$ NMR (202 MHz $\text{C}_6\text{H}_5\text{F}$): δ 179.45 (d, $J_{\text{RHP}} = 263$ Hz, 2P). $^{19}\text{F}\{^1\text{H}\}$ NMR (282 MHz $\text{C}_6\text{H}_5\text{F}$): δ -120.5 (s ($\text{C}_6\text{H}_5\text{F}$), F), -62.5 (s (BAR^{F_4}), 24F). ESI-MS: $[\text{M}^+]$ $m/z = 525.12$, $[\text{M}^+]$ calc = 525.12 (correct isotope pattern). Elemental Micro-Analysis: $\text{C}_{52}\text{H}_{49}\text{BF}_{25}\text{O}_4\text{P}_2\text{Rh}$ C, 44.98H, 3.56 found C, 44.80H, 3.84.

$\text{Rh}\{(\text{O}^i\text{Pr}_2)\text{PCH}_2\text{CH}_2\text{P}(\text{O}^i\text{Pr}_2)\}(\text{NBD})[\text{BAR}^{\text{F}_4}]$

90 mg (195 mmol) of $[(\text{NBD})\text{RhCl}]_2$ was added to a Schlenk tube with a stirrer bar and dissolved in 5 ml of $\text{C}_6\text{H}_5\text{F}$. To this, 3 ml of a 0.131 M (393 mmol, 2 eq.) of a pentane solution of (O^iPr_2) $\text{PCH}_2\text{CH}_2\text{P}(\text{O}^i\text{Pr}_2)$ was added and the mixture stirred for 5 min, a slight darkening of the yellow solution is observed. This mixture was added to a Schlenk flask containing 346.2 mg (391 mmol) Na $[\text{BAR}^{\text{F}_4}]$ and a moving stirrer bar by cannula transfer to give an orange solution. The solvent was reduced by vacuum to 1 ml and 10 ml of pentane was added. A stream of argon bubbles was passed through the mixture to aid precipitation of the product. The product was dissolved in CH_2Cl_2 and NaCl removed by filter cannula methods. Finally recrystallisation was achieved by layering with pentane (N.B. an oily product is typical, although slow crystallisation occurs over time at 277 K). Yield = 220 mg (41%). ^1H NMR (300 MHz CD_2Cl_2): δ 1.29 (δ (^iPr CH_3), $J_{\text{HH}} = 6$ Hz, 12H), 1.33 (d (^iPr CH_3), $J_{\text{HH}} = 6$ Hz, 12H), 1.86 (d ($\text{PCH}_2\text{CH}_2\text{P}$), $J_{\text{PH}} = 22$ Hz, 4H), 1.88 (m (NBD CH_2), 2H), 4.17 (s (NBD bridgehead), 2H), 4.42 (m (OCHMe_2), 4H), 5.91 (s (NBD $\text{C}=\text{C}$), 4H), 7.56 (s (BAR^{F_4}), 4H), 7.72 (s (BAR^{F_4}), 8H). $^{31}\text{P}\{^1\text{H}\}$ NMR (122 MHz CD_2Cl_2): δ 167.30 (d, $J_{\text{RHP}} = 217$ Hz, 2P). ESI-MS: $[\text{M}^+]$ $m/z = 537.15$, $[\text{M}^+]$ calc = 537.14 (correct isotope pattern). Elemental Micro-Analysis: $\text{C}_{53}\text{H}_{52}\text{BO}_4\text{F}_{24}\text{P}_2\text{Rh}$ C, 45.97H, 3.79 found C, 45.95H, 3.81.

Single Crystal X-Ray Diffraction. Single crystal X-ray diffraction data for **16** were collected using an Agilent SuperNova (Cu $K\alpha$ radiation, $\lambda = 1.54180$ Å) with the use of low temperature devices. Data were reduced using the instrument manufacturer software, CrysAlisPro [63]. The structure was solved *ab initio* using SIR92 [64], and refined using CRYSTALS [65,66]. Refinement details for **16**: On initial refinement disorder was located in two of the O^iPr groups;

both were modelled over two sites (one disorder model hinging at the O, the other at the P atom). Restraints were used to maintain sensible geometries. The C_6H_5F ligand was also disordered with the fluorine atom located in 3 different positions around the ring. The carbons were, however, ordered and did not need further modelling. The fluorine/hydrogen occupancies were modelled appropriately over the three disorder positions. Several of the CF_3 groups upon the anion were modelled over two positions and restrained to maintain sensible geometries.

Acknowledgement

The EPSRC and the University of Oxford for funding (DTG and PhD Plus Doctoral Prize Award to SDP). The Royal Society for an International Collaboration Travel Grant (ASW JSM). NSERC, CFI and the University of Victoria for operational and infrastructural funding (JSM). Johnson Matthey for the loan of rhodium salts.

Appendix A. Supplementary material

CCDC 1014324 contains the supplementary crystallographic data for this paper. These data can be obtained free of charge from Cambridge Crystallographic Data Centre via www.ccdc.cam.ac.uk/data_request/cif.

Appendix B. Supplementary data

Supplementary data related to this article can be found at <http://dx.doi.org/10.1016/j.jorganchem.2014.08.012>.

References

- J.F. Hartwig, *OrganoTransition Metal Chemistry*, University Science Books, 2010.
- A.Y. Verat, M. Pink, H. Fan, J. Tomaszewski, K.G. Caulton, *Organometallics* 27 (2007) 166–168.
- A.B. Chaplin, J.F. Hooper, A.S. Weller, M.C. Willis, *J. Am. Chem. Soc.* 134 (2012) 4885–4897.
- I. Pernik, J.F. Hooper, A.B. Chaplin, A.S. Weller, M.C. Willis, *ACS Catal.* 2 (2012) 2779–2786.
- J.F. Hooper, R.D. Young, A.S. Weller, M.C. Willis, *Chem. Eur. J.* 19 (2013) 3125–3130.
- J.F. Hooper, R.D. Young, I. Pernik, A.S. Weller, M.C. Willis, *Chem. Sci.* 4 (2013) 1568–1572.
- R. Dallanegra, A.P.M. Robertson, A.B. Chaplin, I. Manners, A.S. Weller, *Chem. Commun.* 47 (2011) 3763–3765.
- T.M. Douglas, A.B. Chaplin, A.S. Weller, X. Yang, M.B. Hall, *J. Am. Chem. Soc.* 131 (2009) 15440–15456.
- T.N. Hooper, M.A. Huertos, T. Jurca, S.D. Pike, A.S. Weller, I. Manners, *Inorg. Chem.*, 53 3716–3729.
- M.A. Huertos, A.S. Weller, *Chem. Sci.* 4 (2013) 1881–1888.
- R. Dallanegra, A.B. Chaplin, A.S. Weller, *Angew. Chem. Int. Ed.* 48 (2009) 6875–6878.
- R. Dallanegra, B.S. Pilgrim, A.B. Chaplin, T.J. Donohoe, A.S. Weller, *Dalton Trans.* 40 (2011) 6626–6628.
- T.M. Douglas, S.K. Brayshaw, R. Dallanegra, G. Kociok-Köhn, S.A. Macgregor, G.L. Moxham, A.S. Weller, T. Wondimagegn, P. Vadivelu, *Chem. Eur. J.* 14 (2008) 1004–1022.
- A.B. Chaplin, A.I. Poblador-Bahamonde, H.A. Sparkes, J.A.K. Howard, S.A. Macgregor, A.S. Weller, *Chem. Commun.* (2009) 244–246.
- For further selected examples for fluoroarene complexes see: (a) S.T.H. Willems, P.H.M. Budzelaar, N.N.P. Moonen, R. de Gelder, J.M.M. Smits, A.W. Gal, *Chem. Eur. J.* 8 (2002) 1310–1320; (b) A.K. Renfrew, A.D. Phillips, E. Tapavicza, R. Scopelliti, U. Rothlisberger, P.J. Dyson, *Organometallics* 28 (2009) 5061–5071; (c) C.Y. Tang, J. Lednik, D. Vidovic, A.L. Thompson, S. Aldridge, *Chem. Commun.* 47 (2011) 2523–2525; (d) M.D. Palacios, M.C. Puerta, P. Valerga, A. Lledós, E. Veilly, *Inorg. Chem.* 46 (2007) 6958–6967; (e) H. Lei, J.C. Fettinger, P.P. Power, *Inorg. Chem.* 51 (2012) 1821–1826; (f) A. Higelin, U. Sachs, S. Keller, I. Krossing, *Chem. Eur. J.* 18 (2012) 10029–10034.
- R.J. Kulawiec, R.H. Crabtree, *Coord. Chem. Rev.* 99 (1990) 89–115.
- F. Basuli, H. Aneetha, J.C. Huffman, D.J. Mindiola, *J. Am. Chem. Soc.* 127 (2005) 17992–17993.
- M.W. Bouwkamp, P.H.M. Budzelaar, J. Gercama, I. Del Hierro Morales, J. de Wolf, A. Meetsma, S.I. Troyanov, J.H. Teuben, B. Hessen, *J. Am. Chem. Soc.* 127 (2005) 14310–14319.
- X. Li, J. Baldamus, M. Nishiura, O. Tardif, Z. Hou, *Angew. Chem. Int. Ed. Engl.* 45 (2006) 8184–8188.
- C.L. Higgitt, A. Hugo Klahn, M.H. Moore, B. Oelckers, M.G. Partridge, R.N. Perutz, *J. Chem. Soc. Dalton Trans.* (1997) 1269–1280.
- E. Clot, B. Oelckers, A.H. Klahn, O. Eisenstein, R.N. Perutz, *Dalton Trans.* (2003) 4065–4074.
- J.M. Slattery, A. Higelin, T. Bayer, I. Krossing, *Angew. Chem. Int. Ed.* 49 (2010) 3228–3231.
- E. Clot, O. Eisenstein, N. Jasim, S.A. Macgregor, J.E. McGrady, R.N. Perutz, *Acc. Chem. Res.* 44 (2011) 333–348.
- S.D. Pike, A.L. Thompson, A.G. Algarra, D.C. Apperley, S.A. Macgregor, A.S. Weller, *Science* 337 (2012) 1648–1651.
- T.M. Douglas, E. Molinos, S.K. Brayshaw, A.S. Weller, *Organometallics* 26 (2006) 463–465.
- J. Powell, A. Lough, T. Saeed, *J. Chem. Soc. Dalton Trans.* (1997) 4137–4138.
- P. Dierkes, P.W.N.M. Van Leeuwen, *J. Chem. Soc. Dalton Trans.* (1999) 1519–1530.
- P.W.N.M. Van Leeuwen, P.C.J. Kamer, J.N.H. Reek, P. Dierkes, *Chem. Rev.* 100 (2000) 2741–2770.
- T.K. Trefz, M.A. Henderson, M.Y. Wang, S. Collins, J.S. McIndoe, *Organometallics* 32 (2013) 3149–3152.
- V. Ryzhov, C.-N. Yang, S.J. Klippenstein, R.C. Dunbar, *Int. J. Mass Spectrom.* 185–187 (1999) 913–923.
- F. Meyer, F.A. Khan, P.B. Armentrout, *J. Am. Chem. Soc.* 117 (1995) 9740–9748.
- C.W. Bauschlicher Jr., H. Partridge, *Chem. Phys. Lett.* 181 (1991) 129–133.
- W. Henderson, J.S. McIndoe, *Mass Spectrometry of Inorganic and Organometallic Compounds*, John Wiley and Sons, Chichester, 2005.
- E. Crawford, J.S. McIndoe, D.G. Tuck, *Can. J. Chem.* 84 (2006) 1607–1613.
- J.B. Fenn, M. Mann, C.K. Meng, S.F. Wong, C.M. Whitehouse, *Mass Spectrom. Rev.* 9 (1990) 37–70.
- K.L. Vikse, M.P. Woods, J.S. McIndoe, *Organometallics* 29 (2010) 6615–6618.
- L.P.E. Yunker, R.L. Stoddard, J.S. McIndoe, *J. Mass Spectrom.* 49 (2014) 1–8.
- A.T. Lubben, J.S. McIndoe, A.S. Weller, *Organometallics* 27 (2008) 3303–3306.
- S. Torke, D. Merki, P. Chen, *J. Am. Chem. Soc.* 130 (2008) 4808–4814.
- E.P.A. Couzijn, E. Zocher, A. Bach, P. Chen, *Chem. Eur. J.* 16 (2010) 5408–5415.
- I.J. Kobylanski, F.J. Widner, B. Kräutler, P. Chen, *J. Am. Chem. Soc.* 135 (2013) 13648–13651.
- S.D. Pike, A.S. Weller, *Dalton Trans.* 42 (2013) 12832–12835.
- A. Woolf, A.B. Chaplin, J.E. McGrady, M.A.M. Alibadi, N. Rees, S. Draper, F. Murphy, A.S. Weller, *Eur. J. Inorg. Chem.* (2011) 1614–1625.
- P. Pregosin, *NMR in Organometallic Chemistry*, Wiley-VCH, Weinheim, 2012.
- The decomposition of **9** in CH_2Cl_2 solution hampered the collection of equilibrium data over long periods of time. However cooling complex **5** from 298 K to 248 K and then to 298 K over a total time of 2 hours resulted in no significant change in the equilibrium constant. Nevertheless these data should be taken as qualitative rather than quantitative. Noteworthy is that other $[BAR^F_4]$ -coordinated systems take significantly longer to reach equilibrium when in exchange with other weakly coordinating anions, see reference [25].
- N.S. Townsend, A.B. Chaplin, M.A. Naser, A.L. Thompson, N.H. Rees, S.A. Macgregor, A.S. Weller, *Chem. Eur. J.* 16 (2010) 8376–8389.
- M. Brookhart, M.L.H. Green, G. Parkin, *Proc. Natl. Acad. Sci. U S A* 104 (2007) 6908–6914.
- X.-L. Luo, G.J. Kubas, C.J. Burns, R.J. Butcher, J.C. Bryan, *Inorg. Chem.* 34 (1995) 6538–6545.
- N. Hao, M.J. McGlinchey, *J. Organomet. Chem.* 165 (1979) 225–231.
- N. Hao, M.J. McGlinchey, *J. Organomet. Chem.* 161 (1978) 381–390.
- K.J. Klabunde, H.F. Efner, *Inorg. Chem.* 14 (1975) 789–791.
- A. Agarwal, M.J. McGlinchey, T.-S. Tan, *J. Organomet. Chem.* 141 (1977) 85–97.
- T. Albright, J. Burdett, M. Whangbo, *Orbital Interactions in Chemistry*, Wiley, Hoboken, New Jersey, 2013.
- T.M. Douglas, A.B. Chaplin, A.S. Weller, *Organometallics* 27 (2008) 2918–2921.
- A. Carter, S.A. Cohen, N.A. Cooley, A. Murphy, J. Scutt, D.F. Wass, *Chem. Commun.* (2002) 858–859.
- L.E. Bowen, M. Charernsuk, T.W. Hey, C.L. McMullin, A.G. Orpen, D.F. Wass, *Dalton Trans.* 39 (2010) 560–567.
- H. Urtel, C. Meier, F. Rominger, R. Hofmann, *Organometallics* 29 (2010) 5496–5503.
- A.B. Pangborn, M.A. Giardello, R.H. Grubbs, R.K. Rosen, F.J. Timmers, *Organometallics* 15 (1996) 1518–1520.
- W.E. Buschmann, J.S. Miller, *Inorg. Synth.* 33 (2002) 83–91.
- M.D. Fryzuk, *Can. J. Chem.* 61 (1983) 1347–1351.
- R.B. King, W.M. Rhee, *Inorg. Chem.* 17 (1978) 2961–2963.
- M. Kranenburg, Y.E.M. van der Burgt, P.C.J. Kamer, P.W.N.M. van Leeuwen, K. Goubitz, J. Fraanje, *Organometallics* 14 (1995) 3081–3089.
- Oxford Diffraction Ltd, Abingdon, England: 2011.
- A. Altomare, G. Cascarano, C. Giacovazzo, A. Guagliardi, M.C. Burla, G. Polidori, M. Camalli, *J. Appl. Crystallogr.* 27 (1994) 435.
- P.W. Betteridge, J.R. Carruthers, R.I. Cooper, K. Prout, D.J. Watkin, *J. Appl. Crystallogr.* 36 (2003) 1487.
- R.I. Cooper, A.L. Thompson, D.J. Watkin, *J. Appl. Crystallogr.* 43 (2010) 1100.